Supplementary Information

New conjugated molecular scaffold based on [2,2]paracyclophane as electron acceptors for organic photovoltaic cells

Yang Yang, Guanxin Zhang, Chenmin Yu, Chang He, Jianguo Wang, Xin Chen, Jingjing Yao, Zitong Liu, Deqing Zhang**

Table of Contents

1. General information

Chemicals were purchased form Alfa-Aesar, Sigma-Aldrich, and used without further purification. Solvents and other common reagents were obtained from Beijing Chemical Co.. 4,7,13,16-Tetraethynyl[2,2]paracyclophane (**3**) , 1,4-diethynyl-2,5-dimethylbenzene (**5**) and **2a** was synthesized according to the literature-reported procedures. [S1,S2,S3]

^{1}H NMR and ^{13}C NMR spectra were measured on a Bruker AVANCE III 400 MHz spectrometer. Elemental analysis of carbon, hydrogen, sulfur and nitrogen was performed on a Carlo Erba model 1160 elemental analyzer. UV-vis absorption spectra were measured with JASCO V-570 UV-Vis spectrophtometer. TGA-DTA measurements were carried out on a SHIMADZU DTG-60 instruments under a dry nitrogen flow, heating from room temperature to 550 ℃, with a heating rate of 10 ℃/min. Cyclic voltammetric measurements were carried out in a conventional three-electrode cell using a Pt working electrode, a Pt counter electrode and a Ag/AgCl (saturated KCl) reference electrode on a computer-controlled CHI660C instruments at room temperature; the scan rate was 100 mV s^{-1}, and *n*-Bu_4NPF_6 (0.1 M) was used as the supporting electrolyte.

The GIXRD data were measured at 1W1A, Beijing Synchrotron Raidation Facility. The thin film surfaces were examined by tapping-mode AFM using Digital Instruments Nanoscope V atomic force microscope in ambient air conditions in the dark. AFM samples and microscopic images were identical to those used in organic solar cells.

2. Synthesis of 1a, 1b, 2b and 4.

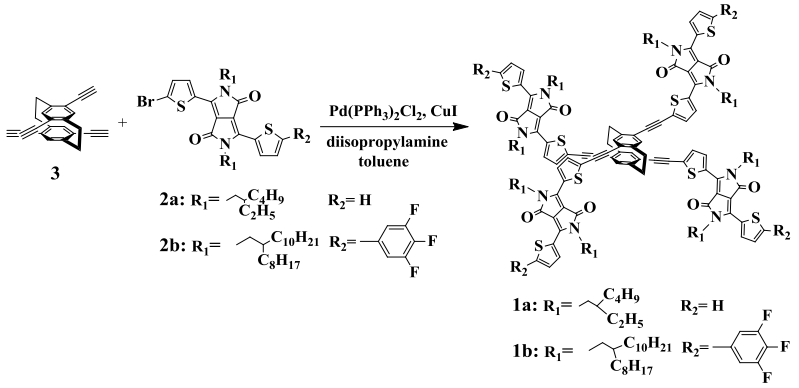

Scheme S1. Synthetic approaches to **1a** and **1b**

Synthesis of 1a. To a degassed toluene solution (25mL) of **3** (30 mg, 0.1 mmol) and **2a** (300 mg, 0.5 mmol), $Pd(PPh_3)_2Cl_2$ (14 mg, 0.02 mmol), CuI (3.8 mg, 0.02 mmol) and diisopropylamine (6.0 mL) was added. The mixture was heated at 75 ^oC for 12 hours under nitrogen atmosphere. After cooling to room temperature, the solvent was evaporated under vacuum and the residue was subjected to silica gel column chromatography with petroleum ether (60-90 ^oC)/CH_2Cl_2 (v/v, 1/1) as eluent. Compound **1a** was obtained as a purple-red solid (35 mg) in 15% yield. ^1H NMR (400 MHz, $CDCl_3$, δ) 8.96 (d, *J* = 3.2 Hz, 4H), 8.90 (d, *J* = 3.2 Hz 4H), 7.64 (d, *J* = 4.9 Hz, 4H), 7.45 (d, *J* = 3.9 Hz, 4H), 7.30 – 7.24 (m, 4H), 7.14 (s, 4H), 4.14 – 3.93 (m, 16H), 3.58 – 3.56 (m, 4H), 3.15-3.11 (m, 4H), 1.89 (br, 8H), 1.36 – 1.25 (m, 64H), 0.92 – 0.86 (m, 48H). ^{13}C NMR (100 MHz, $CDCl_3$, δ): 161.69, 142.36, 141.08, 138.99, 135.86, 135.36, 134.65, 133.08, 131.29, 131.04, 129.91, 128.64, 128.02, 124.93, 109.17, 108.20, 97.01, 88.33, 46.08, 39.39, 39.22, 32.96, 30.36, 28.55, 28.48, 23.75, 23.67, 23.19, 14.19, 14.15, 10.69, 10.62. MALDI-TOF: 2416.5 [$M+K^+$]; Anal. calcd for $C_{144}H_{168}N_8O_8S_8$: C, 72.20; H, 7.07; N, 4.68; S, 10.71; found: C, 71.80; H, 6.90; N, 4.68; S, 10.45.

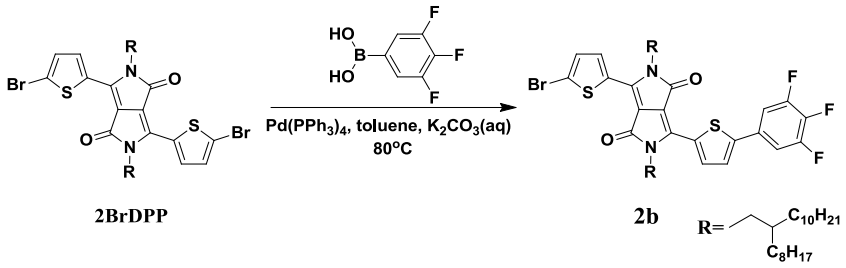

Scheme S2. Synthetic approach to **2b**.

Synthesis of 2b. To the solution of **2BrDPP** (*N*-$C_{20}H_{41}$) (305 mg, 0.30 mmol) and 3,4,5-triflurophenylboronic acid (52 mg, 0.30 mmol) in 20 mL of anhydrous toluene deoxygenated with nitrogen, catalytic amount of $Pd(PPh_3)_4$ was added under nitrogen atmosphere. Aqueous 2.0 M K_2CO_3 (8 mL) and ethanol (3 mL) were added to the above mixture. The mixture was heated at 80°C for 12 hrs under nitrogen atmosphere. After cooling to room temperature, water (40 mL) was added and the mixture was extracted with CH_2Cl_2 (2×40mL). The organic phase was dried over anhydrous $MgSO_4$ and filtered. After removing the solvent from filtrate, the residue was subjected to silica gel column chromatography with petroleum ether (60-90°C)/CH_2Cl_2(v/v, 1/1) as eluent. Compound **2b** was obtained as a purple solid (35 mg) in 50% yield. ^{1}H NMR (400 MHz, CD_2Cl_2 , δ) 8.84 (d, *J* = 4.1 Hz, 1H), 8.63 (d, *J* = 4.1 Hz, 1H), 7.41 (d, *J* = 4.1 Hz, 1H), 7.35 – 7.26 (m, 2H), 7.23 (d, *J* = 4.1 Hz, 1H), 3.98 (d, *J* = 7.6 Hz, 2H), 3.90 (d, *J* = 7.6 Hz, 2H), 1.88 (br, 2H), 1.32 – 1.18 (m, 64H), 0.92 – 0.81 (m, 12H). ^{13}C NMR (100 MHz, CD_2Cl_2 , δ) 161.88, 161.82 , 146.00, 140.06, 139.68, 136.84, 135.75, 132.01, 131.99, 130.82, 126.17, 119.34, 110.92, 110.86, 110.76, 110.69, 109.19, 108.82, 46.81, 46.75, 38.52, 38.37, 32.54, 32.51, 32.48, 31.91, 31.78, 30.62, 30.58, 30.27, 30.26, 30.23, 30.21, 30.16, 30.11, 29.98, 29.96, 29.92, 26.96, 26.77, 23.29, 23.26, 14.48, 14.45. MALDI-TOF: 1070.6 [M+H$^+$]; Anal. calcd for $C_{60}H_{88}F_3N_2O_2S_2$: C, 67.33; H, 8.29; N,2.62; S, 5.99; found: C, 67.47; H,8.28; N, 2.63; S,6.08 .

Synthesis of 1b. **1b** was synthesized similarly with compound **3** and **2b**. Compound **1b** was obtained as a violet solid in 15% yield. ^{1}H NMR (400 MHz, CD_2Cl_2, δ) 8.94 (d, *J* = 3.8 Hz, 4H), 8.90 (d, *J* = 3.8 Hz, 4H), 7.48 (d, *J* = 4.0 Hz, 4H), 7.34 (d, *J* = 4.0 Hz, 4H), 7.30 – 7.21 (m, 8H), 7.20 (s, 4H), 4.02 – 3.85 (m, 16H), 3.60-3.54 (m, 4H), 3.23 – 3.18 (m, 4H), 1.93 (br, 8H), 1.58 – 1.17 (m, 256H), 0.88-0.81 (m, 48H). ^{13}C NMR (100 MHz, $CDCl_3$, δ) 161.61, 150.59, 145.73, 142.14, 139.81, 139.42, 136.71, 135.63, 134.98, 133.02, 131.29, 130.26, 129.48, 128.49, 125.67, 125.22, 121.20, 110.40, 110.17, 109.17, 108.99, 100.14, 98.92, 97.41, 88.43, 55.02, 46.54, 41.99, 38.13, 35.43, 33.01, 32.47, 32.07, 32.02, 31.53, 31.36, 30.75, 30.22, 29.83, 29.79, 29.74, 29.54, 29.51, 29.48, 26.61, 26.45, 22.83, 14.47, 14.26, 9.72, 1.17. MALDI-TOF: 4262.4 [M^+]; Anal. calcd for $C_{264}H_{364}F_{12}N_8O_8S_8$: C, 74.39; H, 8.61; N, 2.63; S, 6.02; found: C, 73.91; H, 8.66; N, 2.64; S, 5.74.

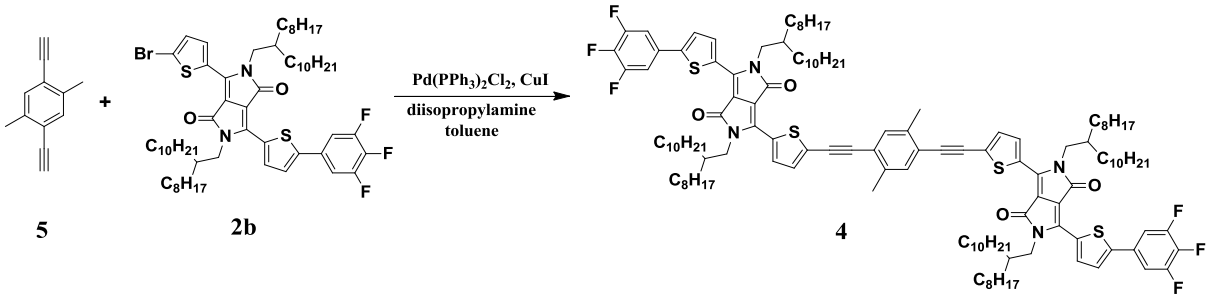

Scheme S3. Synthetic approach to **4**.

Synthesis of 4. **4** was synthesized similarly with compound **5** and **2b**. Compound **5** was obtained as a purple solid in 35% yield. ^{1}H NMR (400 MHz, CD_2Cl_2, δ) 8.92 (d, *J* = 4.1 Hz, 2H), 8.89 (d, *J* = 4.1 Hz, 2H), 7.33 (d, *J* = 4.1 Hz, 2H), 7.29 (d, *J* = 4.1 Hz, 2H), 7.25 (s, 2H), 7.24 – 7.17 (m, 4H), 3.93 – 3.91 (m, 8H), 2.42 (s, 6H), 1.90 (br, 4H), 1.32 –1.22 (m, 128H), 0.88 – 0.82 (m, 24H). ^{13}C NMR (100 MHz, $CDCl_3$, δ) 161.59, 161.51, 153.02, 152.96, 150.57, 150.53, 150.47, 145.62, 141.23, 139.68, 139.45, 138.69, 137.57, 136.61, 135.80, 132.97, 132.68, 130.82, 130.18, 129.44, 128.71, 125.60, 122.87, 110.36, 110.30, 110.19, 110.13,

108.91, 108.83, 100.12, 96.94, 88.04, 46.52, 46.44, 38.09, 37.97, 32.08, 32.07, 32.04, 32.01, 31.48, 31.37, 30.21, 29.84, 29.82, 29.81, 29.78, 29.73, 29.70, 29.53, 29.51, 29.47, 26.57, 26.40, 22.84, 22.82, 22.80, 20.18, 14.26, 14.24. MALDI-TOF: 2133.7 [M^+]; Anal. calcd for $C_{132}H_{184}F_6N_4O_4S_4$: C, 74.32; H, 8.69; N, 2.63; S, 6.01; found: C, 74.25; H, 8.86; N, 2.68; S, 5.96.

3. TGA analysis of 1a, 1b and 4

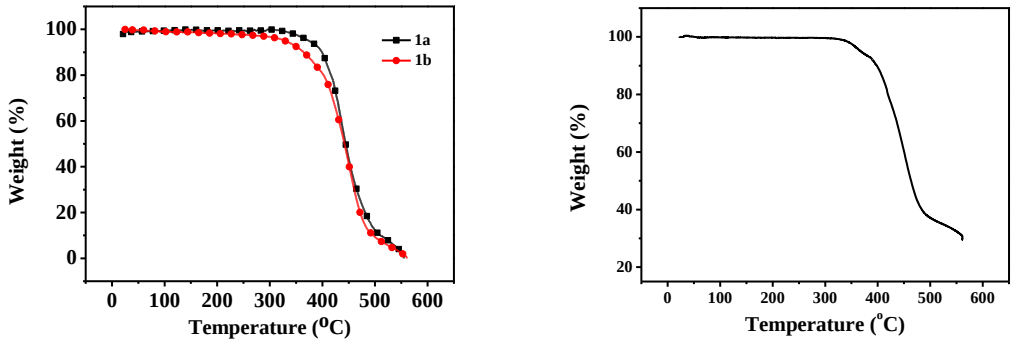

Figure S1. TGA curves of **1a**, **1b** (left) and **4** (right).

4. Cyclic voltammograms, absorption spectra, HOMO/LUMO energies and band gaps of 1a, 1b and 4.

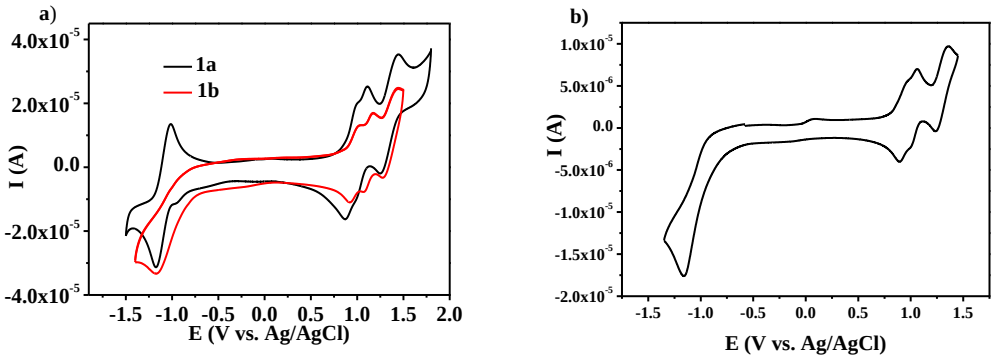

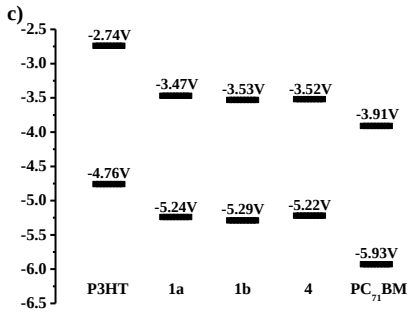

Figure. S2. a) Cyclic voltammograms of **1a** and **1b** in CH_2Cl_2 (1.0×10^{-3} M) at a scan rate of 100 mV/s with n-Bu_4NPF_6 (0.1 M) as the supporting electrolyte; b) Cyclic voltammograms of **4** in CH_2Cl_2 (1.0×10^{-3} M) at a scan rate of 100 mV/s with n-Bu_4NPF_6 (0.1 M) as the supporting electrolyte; c) HOMO/LUMO energies for **1a**, **1b**, **4**, **P3HT** and **$PC_{71}BM$**.

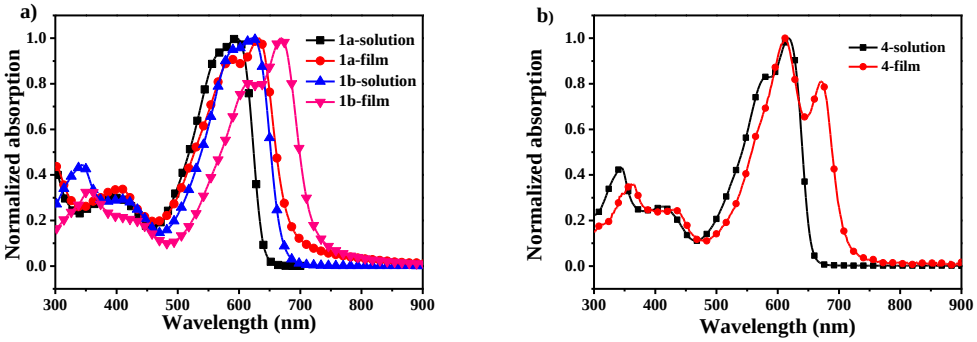

Figure. S3. a) The normalized absorption spectra for solutions of **1a** (1.0×10^{-5}M in CH_2Cl_2) and **1b** (1.0×10^{-5}M in CH_2Cl_2) and their thin films; b) The normalized absorption spectra for solutions of **4** (1.0×10^{-5}M in CH_2Cl_2) and its thin film.

Table S1. Absorption maxima, redox potentials, HOMO/LUMO energies and band gaps of **1a**, **1b** and **4**.

compounds	λ_{max} [nm] solution [a]	film	E_{onset}^{ox1}[V] [f]	E_{onset}^{red1} [V] [f]	HOMO [eV] [c]	LUMO [eV] [c]	band gap [eV]
1a	598 (196300) [b]	631	0.83	-0.94	-5.24	-3.47	1.80 [d] (1.77) [e]
1b	586, 631(154900) [b]	617, 669	0.88	-0.88	-5.29	-3.53	1.70 [d] (1.76) [e]
4	578, 617 (99800) [b]	612, 670	0.81	-0.89	-5.22	-3.52	1.74 [d] (1.70) [e]

[a] Measured in CH_2Cl_2 solutions for **1a**, **1b** and **4** with a concentration of 1.0×10^{-5} M; [b] molar extinction coefficient (ε_{max}, M^{-1} cm^{-1}); [c] calculated based on the respective onset oxidation and reduction potentials of **1a** and **1b** with the following equations: HOMO = − (E_{onset}^{ox}+ 4.41) eV , LUMO = − (E_{onset}^{red}+ 4.41) eV; [d] based on the onset absorption data of thin films; [e] based on the redox potentials. [f] Measured in CH_2Cl_2 solutions for **1a**, **1b** and **4** with a concentration of 1.0×10^{-3} M

5. Fabrication and characterization of solar cells

Solar cells were fabricated with a general structure of ITO/PEDOT:PSS (30 nm)/active layer/Ca (20 nm)/Al (70 nm). The patterned indium tin oxide (ITO) glass substrates were pre-cleaned by sequential ultrasonic treatments in detergent, deionized water, acetone, and isopropyl, and treated in ultraviolet-ozone chamber (Jelight Company, USA) for 30 min. A thin layer (30 nm) of poly (3,4-ethylenedioxythiophene):poly(styrene sulfonate) (PEDOT:PSS, Baytron P VP AI 4083, Germany) was spin-coated onto ITO glass substrates and baked at 150 ^{o}C for 15 min. Solutions of **P3HT**:**1a** and **P3HT**:**1b** with different weight ratios was separately spin-coated on PEDOT:PSS layer to form the respective photoactive layers (ca. 80-100nm). The thickness of the photoactive layer was measured by Ambios Technology XP-2 profilometer. Calcium (ca. 20 nm) and aluminum (ca. 70 nm) layers were then evaporated onto the surface of active layer under vacuum (ca. 10^{-5} Pa) to form the negative electrode. The active area of the device was 4.0 mm^2. *J*–*V* curves were measured with a computer-controlled Keithley 236 Source Measure Unit. A xenon lamp coupled with AM1.5 solar spectrum filters was used as the light source, and the optical power at the sample was 100 mW cm^{-2}. The incident photon to converted current efficiency (IPCE) spectrum was measured by a Stanford Research Systems model SR830 DSP lock-in amplifier coupled with a WDG3 monochromator and 500 W xenon lamp. All presented data were based on ten devices, and the respective best PCEs were presented.

6. Hole and electron mobilities of the blend films of P3HT:1a and P3HT:1b

The hole and electron mobilities within the blending thin films of **P3HT**:**1a** and **P3HT**:**1b** were measured with the space-charge-limited-current (SCLC) method.[S4] For hole-only and electron-only devices, the structures of ITO/PEDOT:PSS/**P3HT**:**1a** (**1b**) (2:1, w/w)/Au and Mg/**P3HT**:**1a** (**1b**) (2:1, w/w)/Mg were used, respectively. Table S2 lists the hole and electron mobilities of the blending thin films of **P3HT**:**1a** and **P3HT**:**1b** at weight ratios of 2:1 before

and after thermal annealing at 150 °C for 10 min. Hole mobilities are much higher than the respective electron mobilities for both **P3HT**:**1a** and **P3HT**:**1b** thin films, thus hole and electron transporting are not balanced within these thin films. Both hole and electron mobilities increase after thermal annealing. For instance, for **P3HT**:**1b** thin film, μ_h increases from 2.10×10^{-4} $cm^2V^{-1}s^{-1}$ to 5.87×10^{-4} $cm^2V^{-1}s^{-1}$, and μ_e increases from 3.53×10^{-6} $cm^2V^{-1}s^{-1}$ to 2.05×10^{-5} $cm^2V^{-1}s^{-1}$. This agrees well with the observation that photovoltaic performances of **P3HT**:**1a** and **P3HT**:**1b** thin films are improved after thermal annealing (see Table S2). Compared to **P3HT**:**1a** thin film, the blending thin film of **P3HT**:**1b** exhibit higher hole and electron mobilities, in particular after thermal annealing, and the ratio of μ_h/μ_e becomes lower after thermal annealing. These results explain the fact that **P3HT**:**1b** thin film yields higher PCE than **P3HT**:**1a** thin film.

Table S2. The hole mobilities, electron mobilities and ratios of hole mobility to electron mobility of **P3HT**:**1a** (2:1, w/w) and **P3HT**:**1b** (2:1, w/w) without or with thermal annealing.

donor:acceptor	annealing [°C]	μ_h [$cm^2V^{-1}s^{-1}$]	μ_e [$cm^2V^{-1}s^{-1}$]	μ_h/μ_e
P3HT:**1a**	as casted	2.06×10^{-4}	2.18×10^{-6}	94.50
	150	3.71×10^{-4}	4.63×10^{-6}	80.13
P3HT:**1b**	as casted	2.10×10^{-4}	3.53×10^{-6}	59.49
	150	5.87×10^{-4}	2.05×10^{-5}	28.63

7. IPCE spectra of OPVs based on P3HT:1a and P3HT:1b

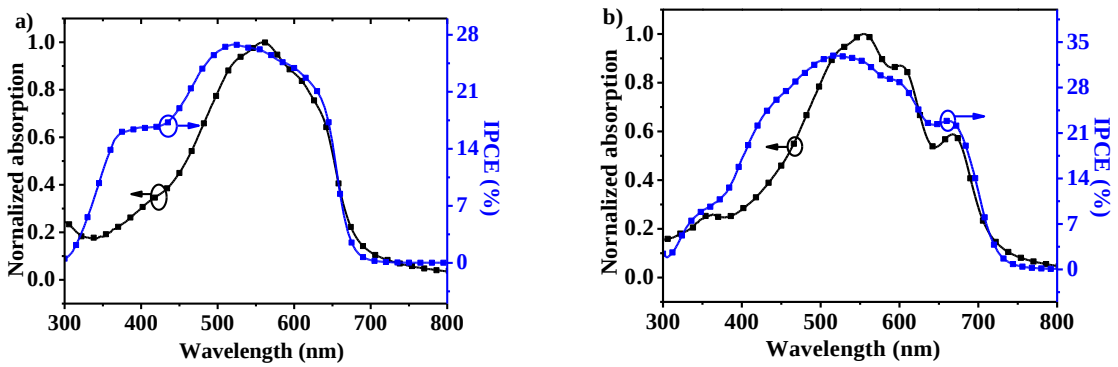

Figure S4. IPCE of OPVs based on **P3HT:1a** (a) and **P3HT:1b** (b), and the corresponding absorption spectra of their thin films at weight ratio of 2:1 after thermal annealing at 150°C for 10 min.

8. XRD patterns and AFM images

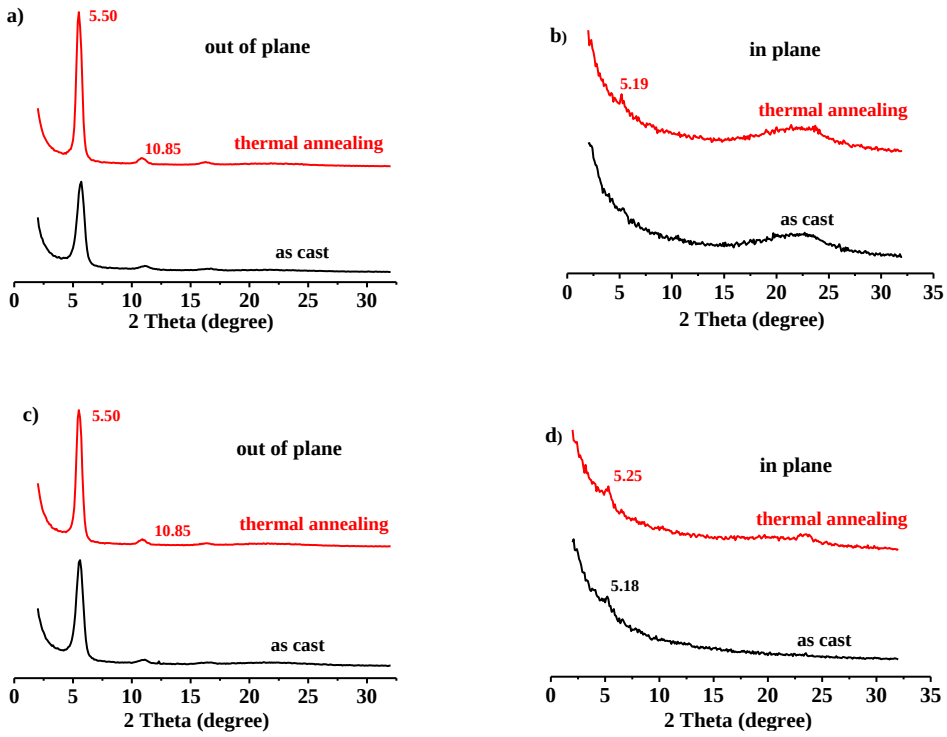

Figure S5. XRD patterns of **P3HT:1a** (2:1, w/w) (a, b) and **P3HT:1b** (2:1, w/w) (c, d) blending films on glass/ITO/PEDOT:PSS substrate before and after thermal annealing.

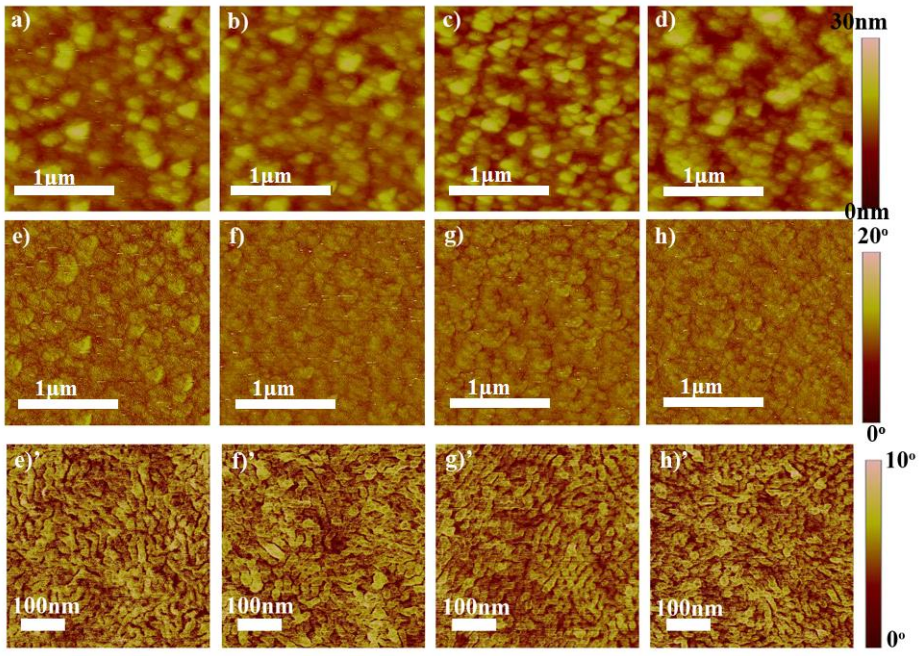

Figure S6. AFM height (a-d) and phase (e-h) images (2 μm×2 μm) of **P3HT**:**1a** (2:1, w/w) blending films without (a, e) and with thermal annealing (b, f) and **P3HT**:**1b** (2:1, w/w) blending films without (c, g) and with thermal annealing (d, h); AFM phase images (500 nm×500 nm) of **P3HT**:**1a** (2:1, w/w) blending films without (e') and with thermal annealing (f') and **P3HT**:**1b** (2:1, w/w) blending films without (g') and with thermal annealing (h').

9. Chemical structures and HOMO/LUMO energies of some typical polymer donors in OPVs

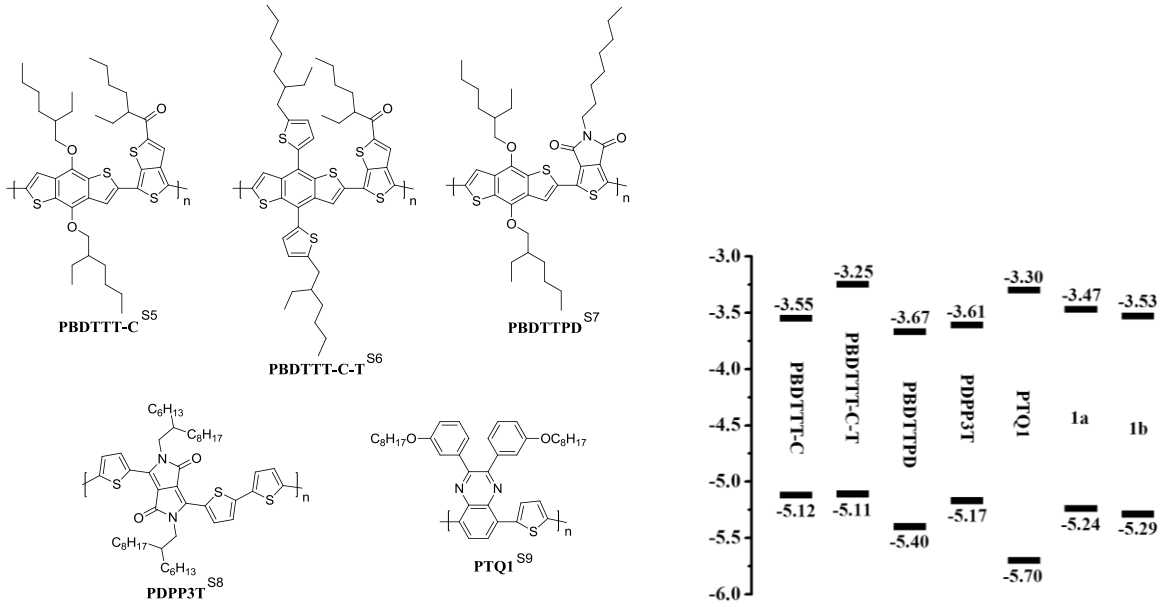

Figure S7 Chemical structures and HOMO/LUMO energies of some typical polymer donors in OPVs.[S5-S9]

References:
S1. L. Bondarenko, I. Dix, H. Hinrichs, H. Hopf, *Sythesis*, 2004, **16**, 2751.
S2. D. McQuade, J. Kim, T. Swager, *J. Am. Chem. Soc.*, 2000, **122**, 5885.
S3. S.Loser, C. Bruns, H. Miyauchi, R. Ortiz, A. Facchetti, S. Stupp, T. Marks, *J. Am. Chem. Soc.*, 2011, **133**, 8142.
S4. G. Malliaras, J. Salem, P. Brock, C. Scott, *Phys. Rev. B*, 1998, **58**, 13411.

S5. J. Hou, H. Chen, S. Zhang, R. Chen, Y. Yang, Y. Wu, G. Li, *J. Am. Chem. Soc.*, 2009, **131**, 15586.
S6. L. Huo, S. Zhang, X. Guo, F. Xu, Y. Li, J. Hou, *Angew. Chem. Int. Ed.*, 2011, **50**, 9697.
S7. C. Piliego, T. Holcombe, J. Douglas, C. Woo, P. Beaujuge, J. Fréchet, *J. Am. Chem. Soc.*, 2010, **132**, 7595.
S8. J. Bijleveld, A. Zoombelt, S. Mathijssen, M. Wienk, M. Turbiez, D. Leeuw, R. Janssen, *J. Am. Chem. Soc.*, 2009, **131**, 16616.
S9. E. Wang, L. Hou, Z. Wang, S. Hellström, F. Zhang, O. Inganäs, M. Andersson, *Adv. Mater.*, **2010**, *22*, 5240.

11. ^{1}H NMR and ^{13}C NMR spectra

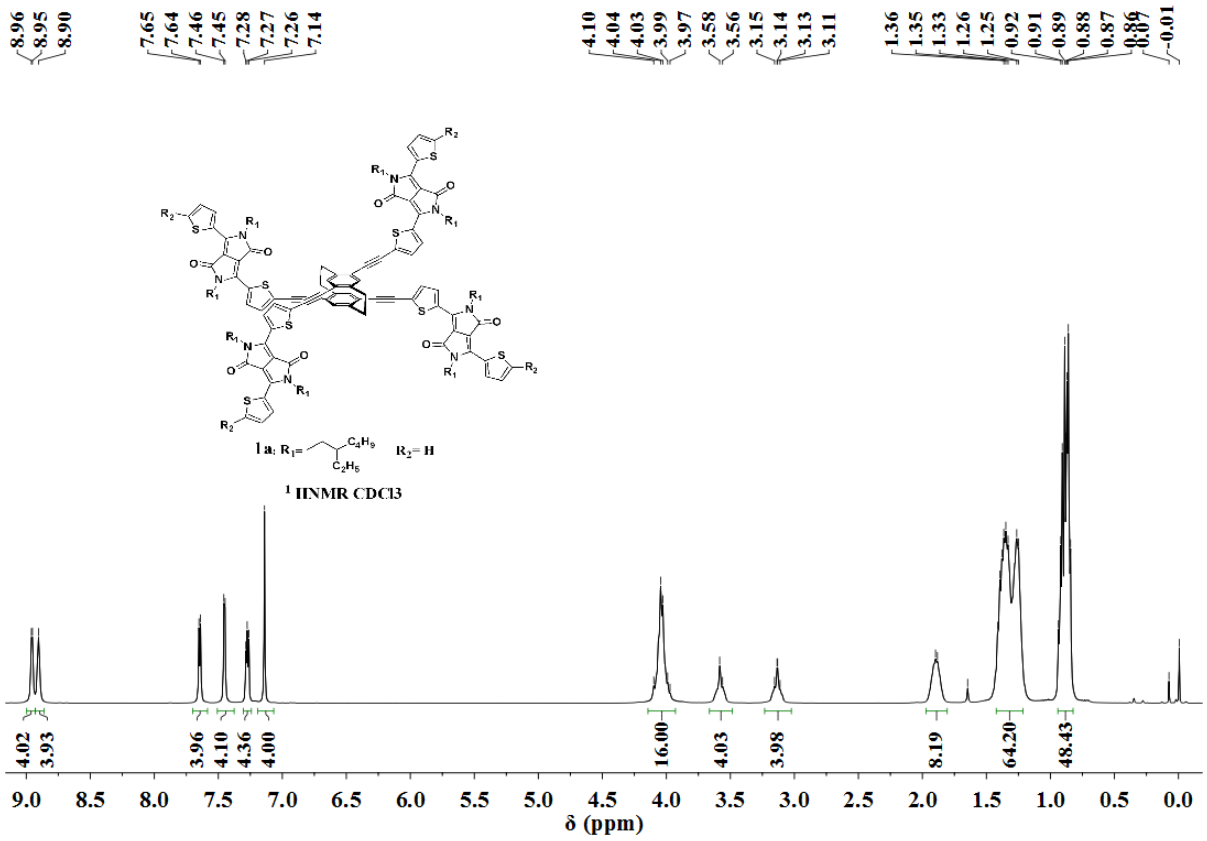

^{1}H NMR of 1a

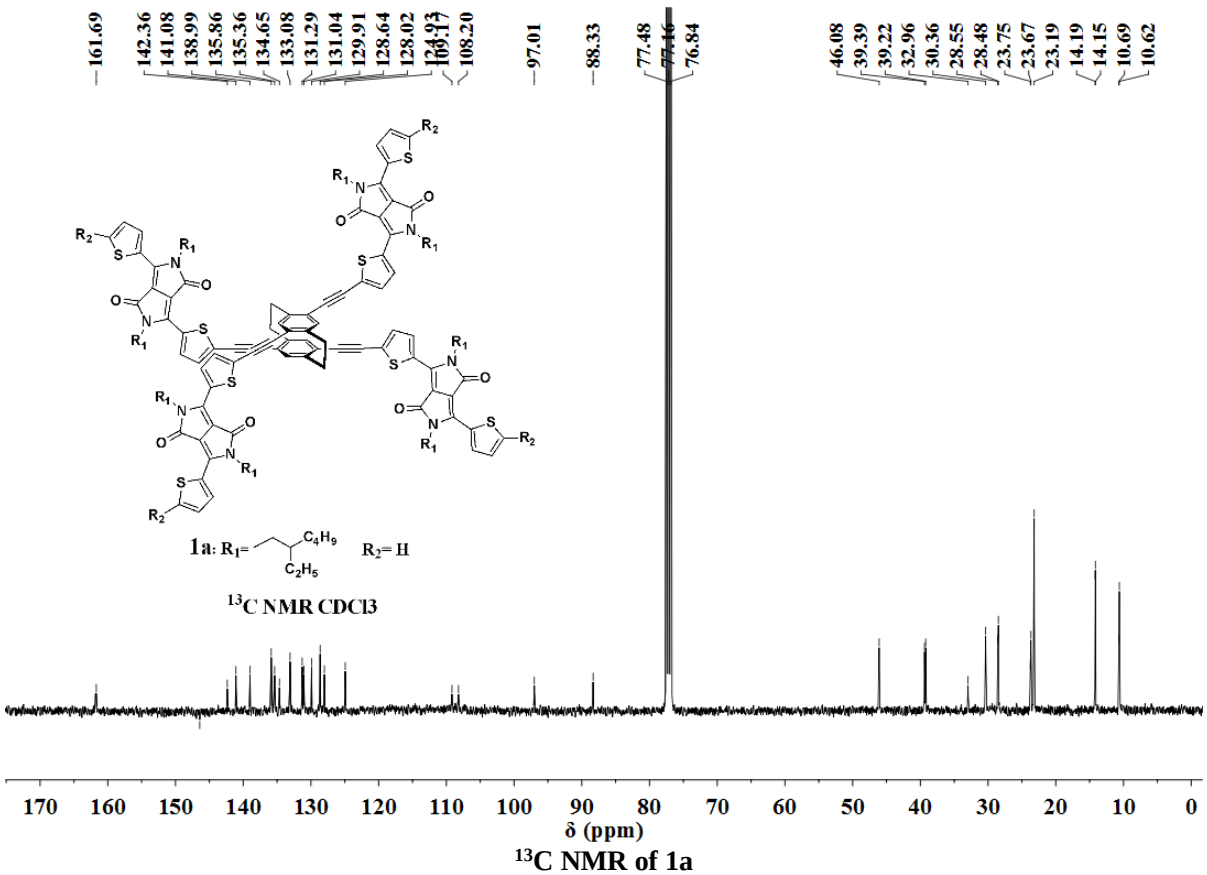

^{13}C NMR of 1a

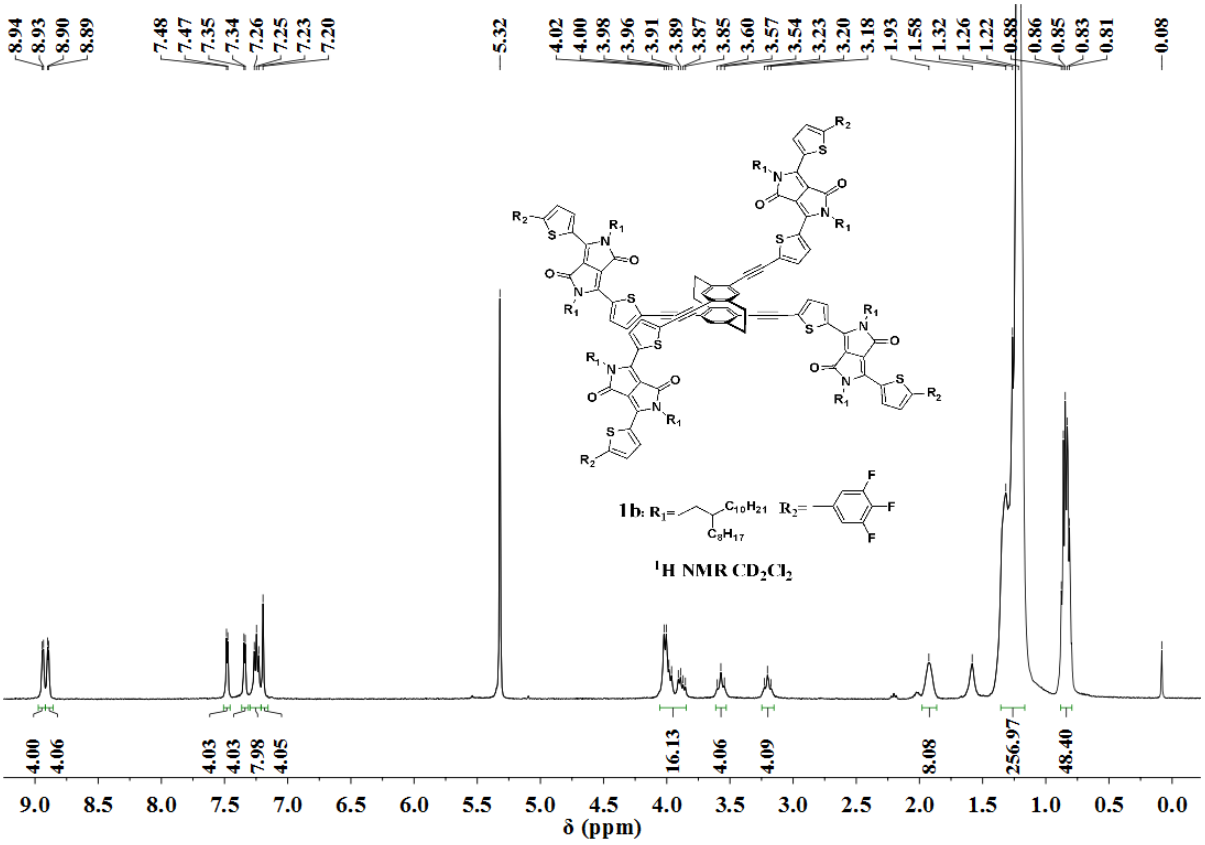

^{1}H NMR of 1b

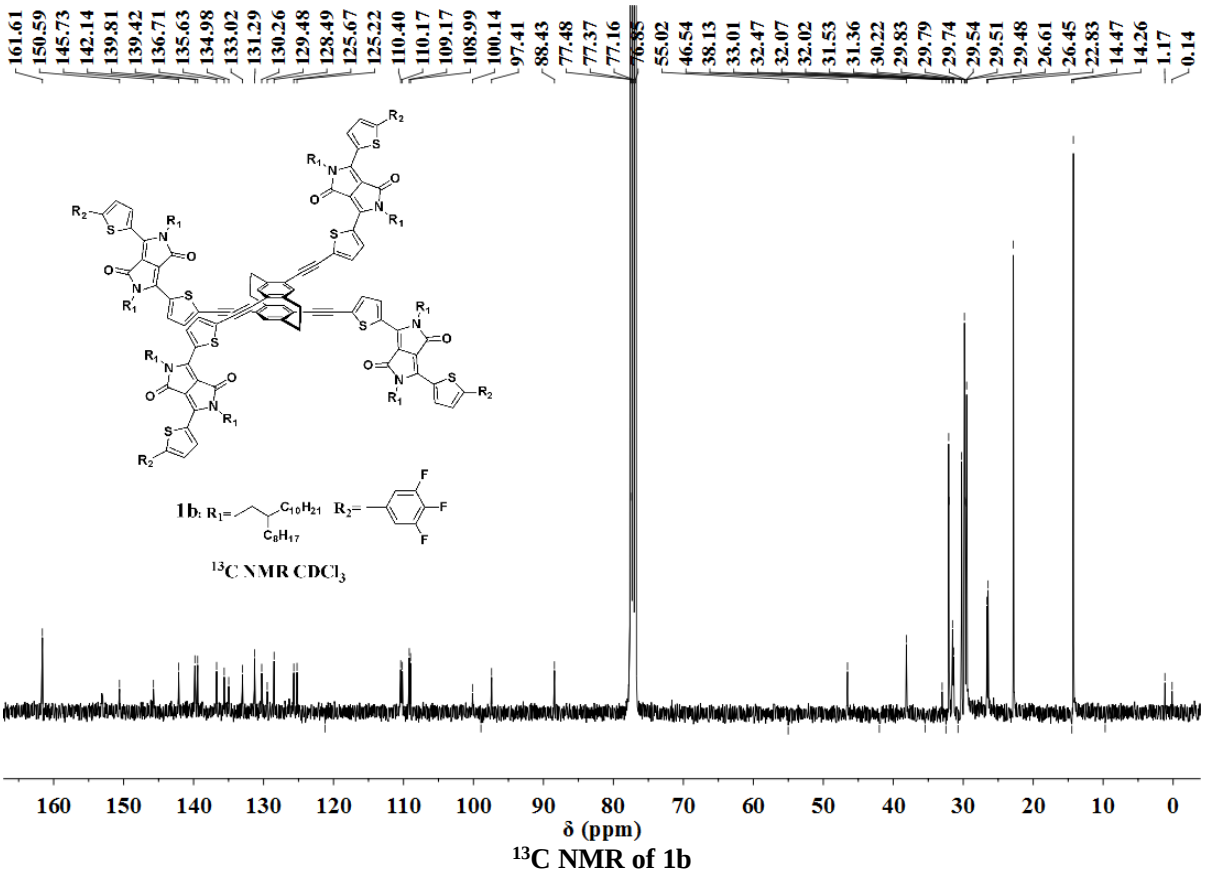

^{13}C NMR of 1b

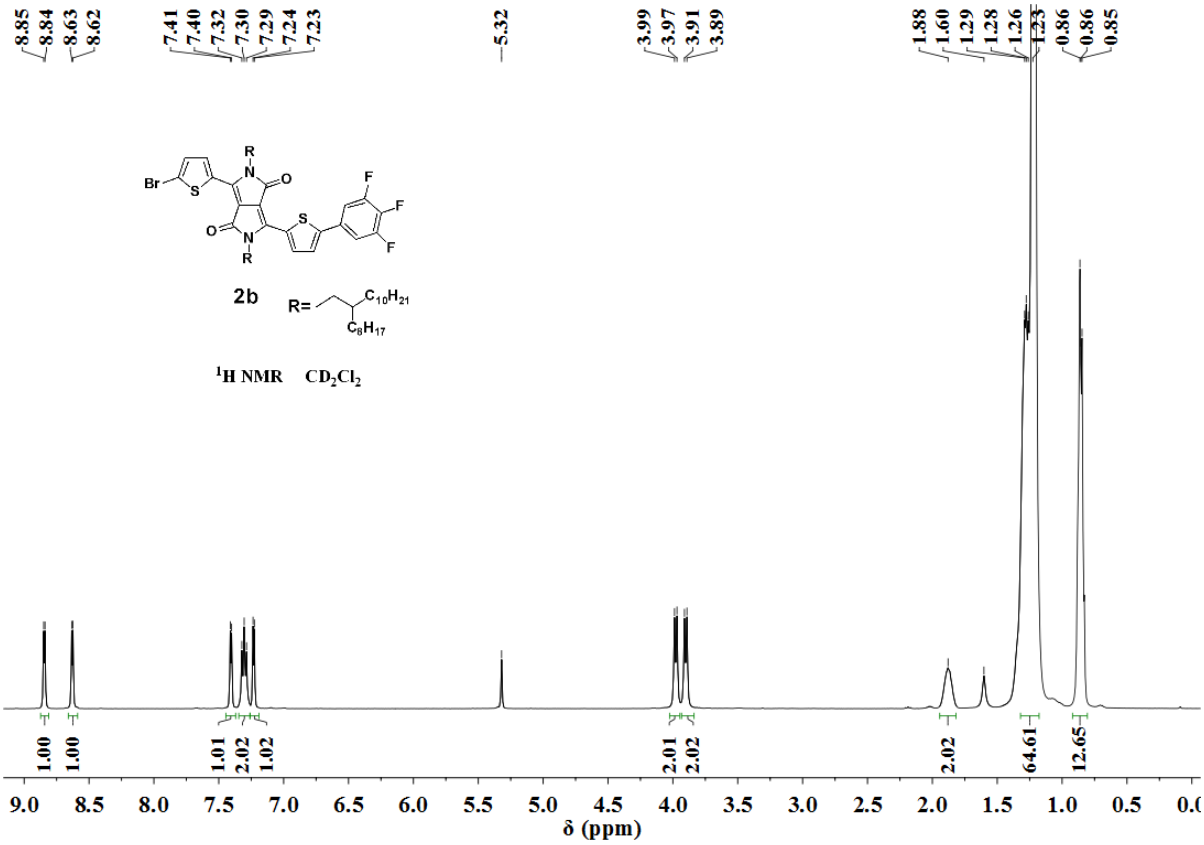

^{1}H NMR of 2b

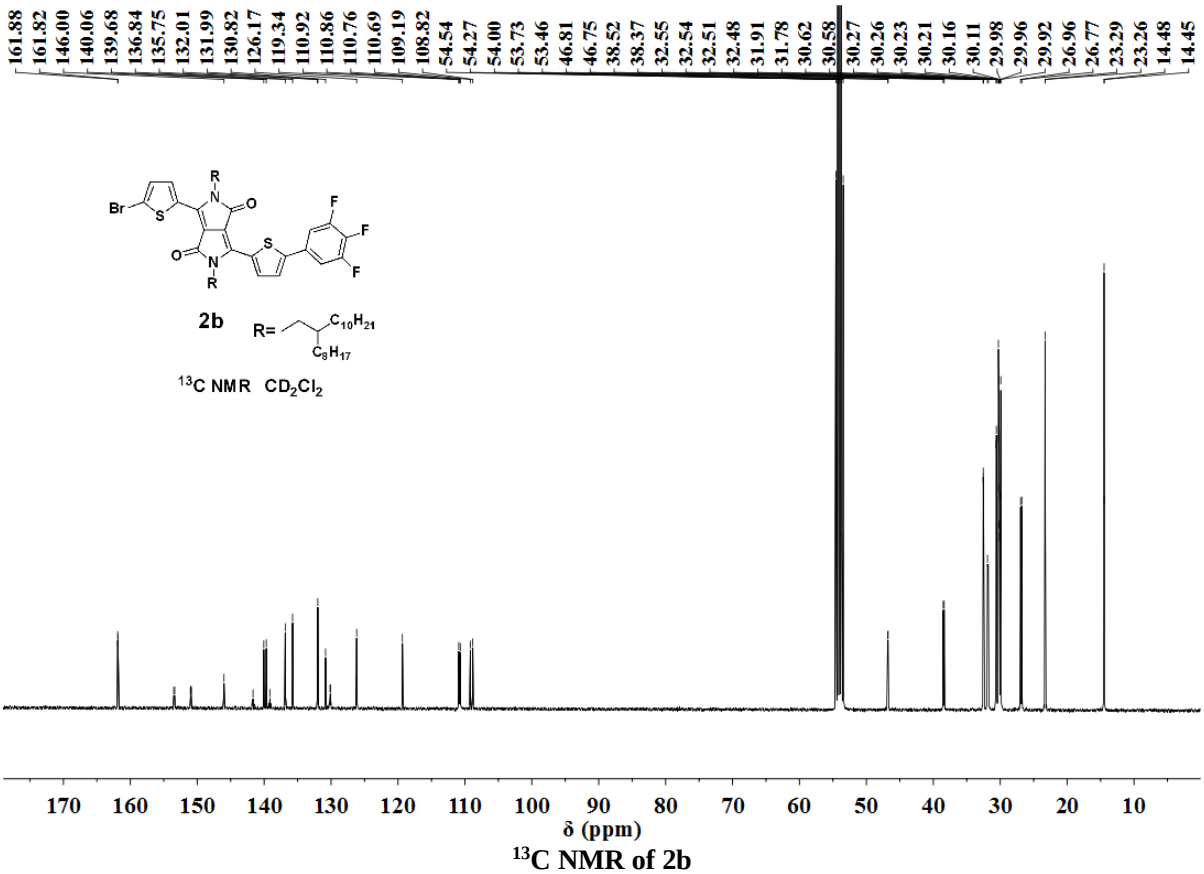

^{13}C NMR of 2b

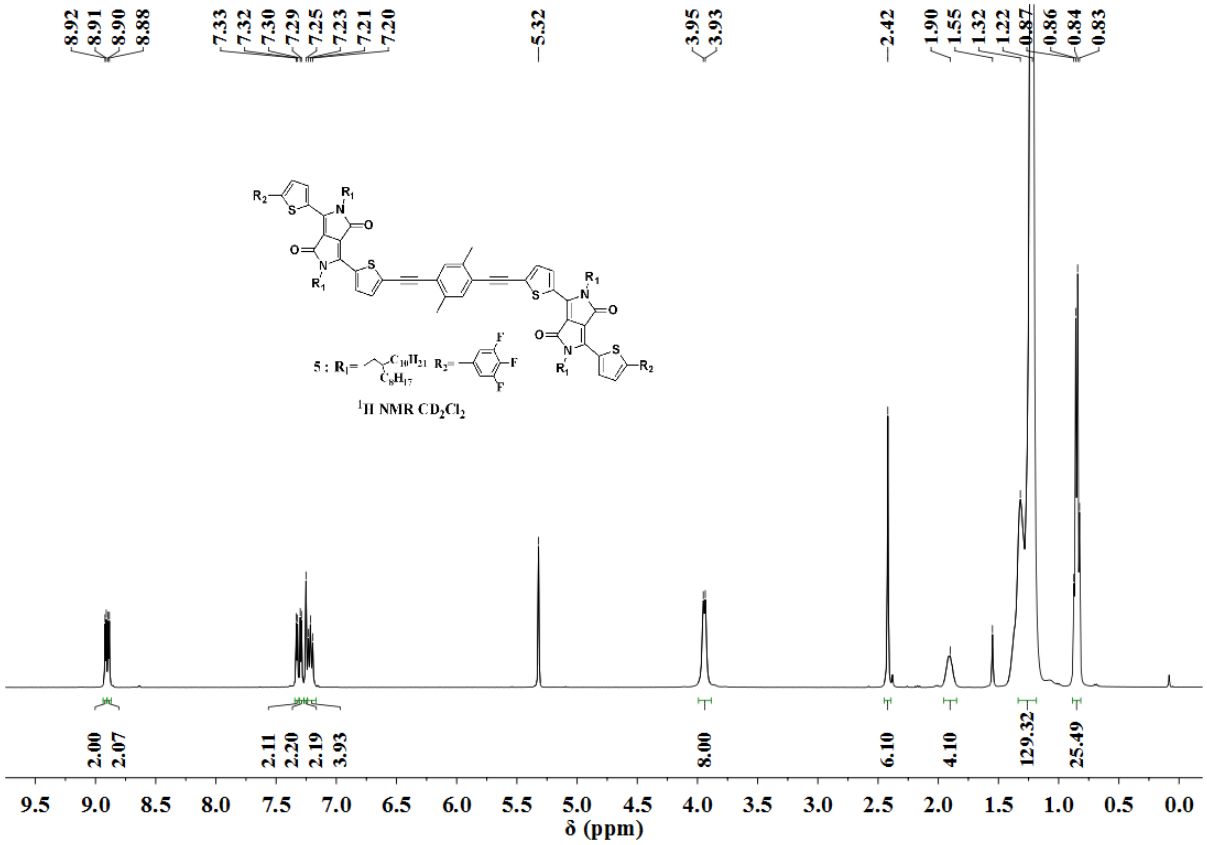

^{1}H NMR of 4

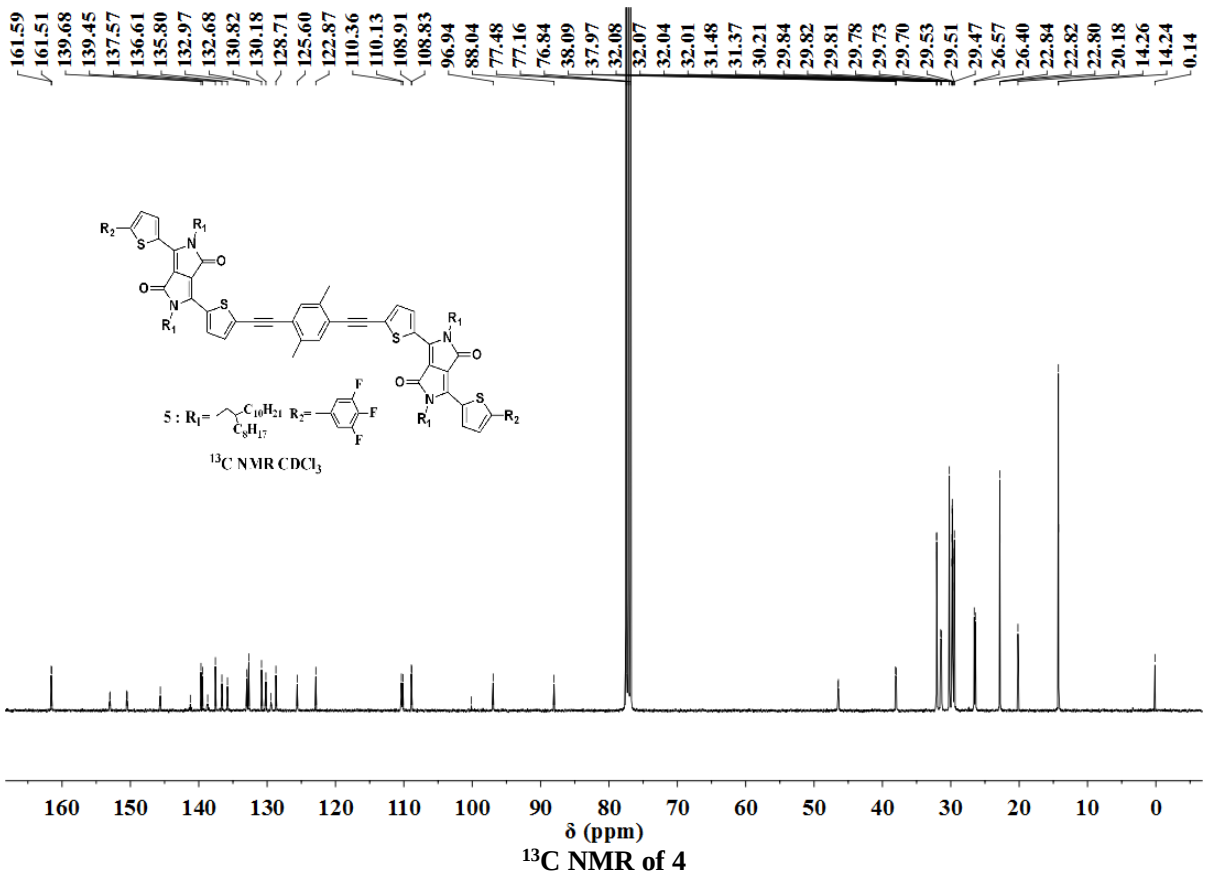

^{13}C NMR of 4